Journal of Magnetic Resonance 210 (2011) 75–81

Contents lists available at ScienceDirect

Journal of Magnetic Resonance

journal homepage: www.elsevier.com/locate/jmr

The influence of the molecular system on the performance of heteronuclear decoupling in solid-state NMR

Guillaume Gerbaud [a,1], Stefano Caldarelli [a,*], Fabio Ziarelli [b], Stéphane Gastaldi [c]

[a] Aix Marseille Université, ISm2 UMR 6263, Campus de Saint Jérôme, Service 511 F-13013 Marseille, France
[b] Spectropole, Fédération de Sciences Chimique de Marseille Université d'Aix Marseille III, Site de Saint Jérôme Service 511, France
[c] Equipe de Chimie Moléculaire Organique, LCP UMR 6264, Boite 562, Université Paul Cézanne, Aix-Marseille III, Faculté des Sciences St Jérôme, Avenue Escadrille Normandie-Niemen, 13397 Marseille Cedex 20, France

ARTICLE INFO

Article history:
Received 3 December 2010
Revised 9 February 2011
Available online 17 February 2011

Keywords:
Solid-state NMR
Heteronuclear decoupling
CPMAS
TPPM
GTn

ABSTRACT

The intensity of the carbon signal in a CPMAS experiment has been measured for two CH and three CH_2 moieties in four test molecules under different phase-modulated proton decoupling conditions and as a function of the spinning rate. The proton decoupling schemes investigated were the golden standard TPPM and three of the GTn family.

Aim of this analysis was to better describe experimentally the impact and limitations of phase-modulated decoupling.

Sizeable differences in the response to decoupling were observed in otherwise chemically identical molecular fragments, such as the $CHCH_2$ found in tyrosine, phenyl-succinic acid or 9-Anthrylmethyl-malonate, probably due to differences in spin-diffusion rates.

In keeping with known facts, the efficiency of the decoupling was observed to decrease with the MAS rate, but with somewhat different trends for the tested systems.

© 2011 Elsevier Inc. All rights reserved.

1. Introduction

The impressive technological advances experienced by NMR of solids may induce the vision of a natural convergence of this domain of applications with its relative field, solution-state NMR. In fact, methods from this latter are becoming available for solids while concepts arisen in the solid-state area, such as the use of the anisotropy of the magnetic interactions, are becoming widespread tools in solution studies. However, one should not underestimate the specificities of organic solids, some of which are not yet dominated by the current status of technology. The main factor in cause here is the intimate structure of the proton dipolar coupled network, generically dubbed the proton "bath" in loose analogy with a thermostat. The size and the characteristics of this latter depend on the molecular shape, as well as on the crystal packing. In fact, the proton–proton dipolar interaction dies out relatively slowly, covering a few bond distances [1]. Therefore, an extended number of actor spins are to be taken into account for the description of an organic material. The frequency spectrum of the resulting Hamiltonian is a particularly intertwined combination of contributions from the original coupled spins. This situation is usually described as a "homogeneous" interaction, a term that often translates into a reluctance to be manipulated by RF pulses, due to the facility of exchange of spin polarization terms among the protons (fast spin-diffusion regime) and to the increased rotary resonance conditions available in the overall Hamiltonian. A first consequence arising from this situation is the difficulty to achieve high-resolution proton spectra. Consequently, diluted nuclei are still a major target for NMR in solids.

Thus, proton heteronuclear decoupling remains a crucial and delicate step in NMR spectroscopy of organic solids towards optimum spectral sensitivity and resolution.

To this respect, the influence of the proton bath at the level of heteronuclear decoupling is particularly intriguing. On one hand the proton–proton interaction lends a helpful self-decoupling effect [2], while on the other hand it still hampers a "clean" manipulation of the proton spins by RF pulses. Also, the presence of interferences with the averaging from the proton CSA has been proposed from the very early times [3] to be a further major source of trouble for decoupling. As a consequence, the discovery of effective ways of performing proton decoupling in solids has lagged behind the achievements of solution-state NMR, where the question is basically solved.

A substantial leap forward to this respect has been the introduction of phase/amplitude modulated irradiation techniques [4]. The proposed methods are based on angle or amplitude modulation of

* Corresponding author.
E-mail address: s.caldarelli@univ-cezanne.fr (S. Caldarelli).
[1] Present address: BIP CNRS – UPR 9036, 31, Chemin Joseph Aiguier 13402, Marseille Cedex 20, France.

1090-7807/$ - see front matter © 2011 Elsevier Inc. All rights reserved.
doi:10.1016/j.jmr.2011.02.013

the applied decoupling field [5–18] on symmetry rules [19], or just on experimental searches directly on the spectrometer [20,21].

Although generally convenient and up to the task, these methods have been shown to suffer from the need of parametric optimization for best performances. Hence, a constant effort is observed to produce new experimental decoupling procedures increasingly robust [15,17,22]. This outstanding experimental progress has been accompanied by the search of a theoretical description suitable to reproduce the key aspects of the phase-modulated decoupling, namely their sensitivity (or lack of) to the periodicity and amplitude of the modulation, or to the influence of the irradiation offset.

Theoretical analysis of the behavior of multiparametric decoupling sequences have been performed by several authors [23–27].

The improvement of modulated RF pulses over continuous-wave (CW) irradiation is apparent in numerical simulation, and the positive role of a sizeable proton spin-diffusion was highlighted from the early studies [24]. Multimodal Floquet analysis was applied to try to decode the interplay of the three averaging fields (MAS, the decoupling RF and its modulation). This kind of analysis reveals and quantifies well the destructive interferences of the three fields, showing that the most negative effects on decoupling come from resonances between the RF irradiation and its modulation [23].

Of particular interest, the dominance of the proton CSA Hamiltonian as the limiting factor in determining a largely non-uniform parametric response has been highlighted [23].

The challenge for the experimentalist is to determine whether a single set of parameters can be chosen for a specific experiment to provide acceptable improvement over non-modulated (CW) decoupling.

In fact, most calculations and demonstrations of decoupling methods concern model systems, the current consensus being that the decoupling behavior is mostly influenced by small molecular motifs, typically the immediate surrounding of the target nucleus, while the influence of the extended proton homonuclear couplings (spin-diffusion, spin-bath) has not been assessed exactly.

In fact, the structure of the internal Hamiltonians, as well as their degree of interference, it is likely to be at variations for any combination of spin system, MAS and decoupling conditions, which may have an impact on the optimal parametrization of the decoupling. It is noteworthy that this kind of reasoning led to the development of experimentally optimized continuously modulated decoupling pulses [15,21].

In this context, the reaction of a given molecular site to decoupling is believed to be determined by its multiplicity (thus different for CH_2, CH or CH_3). The role of the surrounding proton spins is usually summarized to a single parameter, for instance the "strength" of the spin bath or the spin-diffusion rate constant. This approximation does provide some agreement with the experimental results, but it does not yield a satisfactory explanation of the spin dynamics, especially because it is not easy to evaluate *a priori* the proton bath parameters for a solid [24].

One important issue for the experimentalist is to know how much effort should be put in the parametric optimization, a task that is particularly demanding for sample with an intrinsic low signal to noise. To this respect, the crucial point is to determine if it is possible to transfer safely a parameter set optimized for a test sample to the case of interest. As a corollary, it is important to assess the intensity gain introduced by of the use of phase-modulated decoupling.

In this work we characterized the heteronuclear decoupling behavior in a few molecular fragment, some of which serve as typical NMR standards for setting up the decoupling conditions and the rest of which bear similar chemical functions, all carrying CH_2 or CH groups. We submitted this ensemble of compounds to a parametric comparison of the decoupling performance of some phase-modulated pulse. The methods tested were the widespread forerunner TPPM and Gaussian-envelope cosine modulations (GTn), which have shown to be more robust than TPPM with respect to the parametric response [15]. The parameter explored were the MAS frequency, the irradiation offset and the ones describing the phase modulation.

2. Materials and methods

All experiments were performed on a Bruker DRX-400 spectrometer at a B_0 field of 9.4 T in a commercial Bruker probehead using 2.5 mm rotors. Cross-polarization experiments were performed with a variable amplitude contact time[28]. The decoupling field was set at 96.0 kHz. All the decoupling pulses were written in a unique shaped pulse, of a duration corresponding to eight modulation periods, in order to minimize the effect of possible deformation of the shape pulse repetition in the pulse timing. Line intensities were measured directly with the spectrometer software. The influence of the CP on the line intensities was taken into account by using a calibration single-pulse carbon experiment for each molecule at any given MAS frequency. The value obtained this way was normalized to the number of carbon-13 moles, deduced by weighing the sample. We arbitrarily set to 1 the value for glycine recorded under MAS at 10 kHz (on-resonance irradiation).

2.1. Samples

The test molecules, as well as the three-letter code used for reference in the text, are depicted in Fig. 1.

Glycine and L-tyrosine hydrochloride salt were obtained from commercial sources, and used as such.

9-Anthrylmethyl-2-^{13}C-malonate was synthesized according to Ref. [29], using 99.9% ^{13}C-enriched diethylmalonate.

Phenyl-succinic acid, selectively ^{13}C labeled at the CH_2 position, was synthesized according to the procedure described in Appendix A. Both labeled compounds were confirmed to be more than 99% enriched by solution-state NMR.

2.2. Decoupling pulse sequences

The sequences used in this work belong to the family of periodically phase-modulated pulses, which can be described in terms of

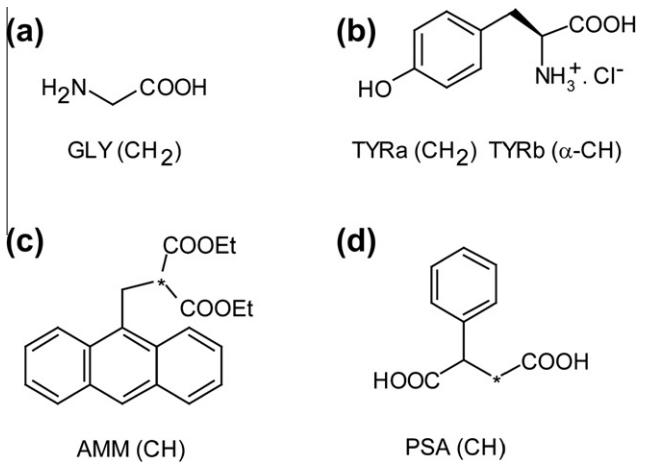

Fig. 1. The samples used in this work, together with the acronyms used throughout the text. (a) Glycine. (b) L-tyrosine hydrochloride. (c) Anthrylmethyl 2-^{13}C malonate. (d) 2-Phenyl-succinic 3-^{13}C acid. The analyzed carbons are the CH and CH_2 elements, indicate by the asterisks for the ambiguous cases.

a fundamental harmonic, ν_{mod}, and of the maximum phase jump, $\Delta\phi$. Two-pulse phase modulation (TPPM), which is a series of pulses of length τ_{mod} and alternating phase $(-\phi_0, \phi_0)$, in this optics corresponds to a square-wave with $\nu_{mod} = 1/(2 * \tau_{mod})$ and $\Delta\phi = 2\phi$. The other decoupling pulses used in this work are constructed as a combination of a Gaussian-envelope, cut at 10% of the maximum intensity, multiplied by the fundamental cosine mode. The consequent broadening induced in the harmonic response has been shown to provide better parametric stability [15]. The broadening can be modulated by varying the number of periods, n, of the fundamental mode spanned by the Gaussian. In this paper we limit our comparison to TPPM and three elements of the GTn family ($n = 2$, 4 and 8).

2.3. Choice of the parameter space

We explored for all molecular systems a decoupling parameter space involving:

- the reduced phase-modulation period, τ_R equals to τ_{mod}/τ_{rf} (thirteen values between 0.3 and 1.5);
- the phase modulation maximum excursion, ϕ_{MAX} (ten values between 0° and 90°);
- the MAS spinning rate (five values from 10 to 30 kHz);
- two values of the irradiation offset, of 2 kHz difference (5 ppm) with respect to each other.

3. Results and discussion

3.1. Pre-characterization of the samples

To evaluate the performance of decoupling on different samples before starting a systematic analysis, we first measured some of the parameters influencing the linewidth of a typical MAS spectrum, recorded with standard but non-optimized decoupling (TPPM with a phase jump of 15°, 10 kHz spinning rate). A thorough analysis of linewidth sources in carbon spectra has been performed by Van der Hart and Campbell [30]. We focus here on two aspects: structural disorder (and in general refocussable broadening) and incomplete proton decoupling. In principle, both components can be assessed via the analysis of a spin-echo indirect detection. Indeed, the effect of this experiment is to produce decay times constants, T_2', unaffected by the resonance dispersion associated to disorder, which influences and often dominates the direct experiment time constant, T_2^*. In the case of non-ideal proton decoupling of organic solids, a more pronounced broadening of the foot rather than of the line as a whole is observed.[24] This can be seen as a signature of a partitioning of the spin system, that is to say the break up of the observed coherences into different reservoirs with characteristic lifetimes. This partition may arise from polymorphism or to be intrinsic to the interaction at play [31,32]. In a spin-echo curve, an effect of this type appears through a multimodal decay, with at least two appreciably distinct time constants. Alternatively, this same effect could be detected in the frequency domain from deviations from "regular" line shapes (i.e. Gaussian or Lorentzian ones) in the signal, if a very good definition of the foot of the line can be achieved [24]. In this preliminary part of the study, the degree of biexponentiality of the spin-echo curve, that is the ratio of the slow and fast component of the decay, has been monitored as one characteristics of the system undergoing decoupling. It should be noted here that, although a biexponential function fits all of our experimental curves, higher partitioning of the lineshape cannot be excluded.

The measurement of the lifetime of the signal of a rare nucleus in an indirect spin-echo experiment holds an interest on its own, as long-lived signals correspond to higher sensitivity of multidimensional experiments [20]. We reported in Table 1 this information in the form of the time, $T_{1/e}$, for which the decay assumes the $1/e$ fractional value of the first point in the echo (taken for $\tau = 0$). For regular, monoexponential time envelopes, $T_{1/e}$ corresponds to T_2'.

All systems, with the exception of AMM, have similar lifetimes. However, glycine and tyrosine spin-echo decays have very little degree of biexponential behavior, compared to PSA and AMM. An analysis of the measured relaxation times (Table 1) points out that these two latter systems are also characterized by much slower relaxation rates, suggesting a possibly different impact of spin-diffusion with respect to glycine and tyrosine chlorohydrate. Indeed, these two molecules have been selected as NMR standards also because of their favorable relaxation properties.

Analysis of Table 1 demonstrates that, consistently with the above discussion, a multi-exponential behavior of the signal decay was observed in many cases. Interestingly, even if the AMM sample is strongly biexponential, a long decay can be still achieved for the signal of this molecule, since the fast decay of its broad component is compensated for by the longest decay time measured for the narrow component.

3.2. Indicators of the decoupling quality

Although the spin-echo method described above constitutes an optimal test for decoupling, it is not a viable one in the case of a systematic study, especially considering the long relaxation times of some of our samples.

The ultimate goals of perfect proton decoupling are better intensity and resolution of the diluted spin spectrum. Linewidth and intensity are thus the natural indicators to monitor decoupling performances. As detailed in the previous section, these two parameters would be totally correlated in an ergodic (i.e. monoexponentially relaxing) system, corresponding to a single Gaussian/Lorentzian line form. In the general case, at any rate, the removal of any broadening interaction has to translate in a direct increase in the signal intensity. The converse, however, could be not true. For instance, this is particularly the case for the contributions arising from the splitting of the signal induced by the presence of modulated perturbations, such as decoupling irradiation and MAS, which appear in the form of multiple sidebands shifted by integer combinations of the RF and spinning frequency [33].

Thus, while linewidths are good descriptors of phenomena affecting markedly the quality of decoupling, the line intensities are better choices to accompany the global process, including the finer effects due to higher order terms of the involved interactions. We shall thus use this latter indicator for describing the decoupling behavior of modulated schemes around their best performance conditions.

3.3. Facility of decoupling of the observed systems

A point that must be addressed in trying to detect any dependence of decoupling on the molecular system is to determine a scale of facility of decoupling. A first indication to this respect comes already from Table 1, by comparison of $T_{1/e}$ and T_{2l}' values, as well as of the biexponentiality degree. It appears that TYR is the easiest system to decouple, followed by GLY. On the other hand, AMM and PSA are the most difficult carbon to decouple.

As a complement of information, continuous-wave decoupling provides the less biased measure of the facility with which a given sample can be decoupled. Moreover, we analyzed the evolution of the linewidth with the MAS rate as a way of characterizing the attitude towards decoupling of the observed systems (Table 2). The values in Table 2 corresponding to MAS at 10 kHz reflect closely the results observed for TPPM (Table 1), with the exception of a inversion of order for PSA and AMM.

Table 1
Spin-echo characterization of the samples under analysis, using TPPM ($\Delta\phi = 15°$) at 10 kHz MAS rate.

	FWHH (Hz)	T_2^* (ms)	$T_{1/e}$[a] (ms)	I_s[b]	I_l[b]	T'_{2s}[b] (ms)	T'_{2l}[b] (ms)	T_{1H} (s)	T_{1C} (s)
GLY CH_2	60	5.3	33	16	84	2.8	40.3	0.4	4.3
TYRa CH_2	27	11.8	32	5	95	1.8	34.5	0.8	62
TYRb α-CH	50	6.4	36	10	90	5.7	39.9	0.7	10
PSA CH_2	90	3.5	34	39	61	5.6	66.9	7.1	302
AMM CH	75	4.2	14	60	40	6.9	42.5	21.8	271

[a] Time for which the spin-echo top has decayed to $1/e$ of the initial value (i.e. for $\tau = 0$).
[b] Result of a biexponential fit to the target function: $I_s\, e^{-t/T2s} + I_l\, e^{-t/T2l}$, where the indexes "l" and "s" stay for "long" and "short", respectively.

Table 2
Evolution of the CW linewidths with the MAS rate for the samples in Fig. 1.

System	MAS (kHz)				
	10	15	20	25	30
GLY CH_2	73	75	85	94	98
TYRa CH_2	42	139	194	295	–
TYRb α-CH	60	62	80	143	217
PSA CH_2	133	161	188	215	262
AMM CH	101	101	102	116	134

The general trend of the carbon linewidth with increasing MAS respects the anticipated degradation, due to reduction of the self-decoupling contribution of the homonuclear proton couplings, although remarkable differences are observed among the five target signals.

The less affected by increasing spinning rates are the CH_2 of GLY and the CH of AMM, which both show moderate increase in the linewidth in going from 10 to 30 kHz MAS rates. In light of the results summarized in Table 1, it is however likely that this similitude is rather driven by opposite trends: a strong, for GLY not really affected by increasing MAS rates, and a weak, for AMM already quenched at moderate MAS rates, self-decoupling effect. The CH_2 signal in TYR broadens with the MAS rate, till beyond detection at 30 kHz spinning rate, while the neighboring CH signal width also broadens significantly. The PSA CH_2 shows an intermediate behavior, doubling its linewidth in going from 10 to 30 kHz. Again, these trends could be qualitatively be used as a rough scale of strength of the proton homonuclear coupling assistance to heteronuclear decoupling.

These results would be surprising if a prevision had to be made on the basis of the main unit, either a CH or a CH_2. An interesting point to note is that PSA, AMM and TYR possess the same CH_2CH fragment. While a precise explanation of the behavior depicted in Table 2 would require an accurate description of the proton Hamiltonian, it appears logical to suggest that the surrounding protons rather than the number of attached ones dominates the decoupling spin dynamics.

3.4. Quantification of the gain in decoupling associated to phase-modulated pulse irradiation and robustness of the decoupling

A practical point that has not attracted the same amount of investigation is the determination of the gain in decoupling efficiency induced by PM methods over CW, which may also be a function of the system under study. This information illustrates firstly whether is worthwhile spending time optimizing the decoupling parameters and secondly provides an experimental insight on the role of the molecular system in the decoupling result. Fig. 2 is a representation of the line intensity produced by TPPM in two systems, GLY and AMM, while varying phase and amplitude of the RF modulation, as well as the MAS rate. The volume encompassed by the drawn surface is the one for which the line intensity is 20% higher than the one produced by CW decoupling. Thus, for GLY at 10 kHz MAS rate TPPM overdoes CW decoupling for a large selection of parameters, up to a maximum of about 150% for the best conditions. On the other end, at 30 kHz spinning rate, while the gain over CW induced by TPPM is much higher at the optimum, only a narrow selection of parameters outperforms the most basic of the decoupling schemes. This volume is a measure of the tolerance of decoupling performance to the settings of the phase modulation. A visual comparison shows that TPPM is worth applying on GLY even for miscalibrated setups, contrary to AMM. Indeed, the case of the AMM system is radically different. While at low spinning rates TPPM does not produces dramatic intensity gains

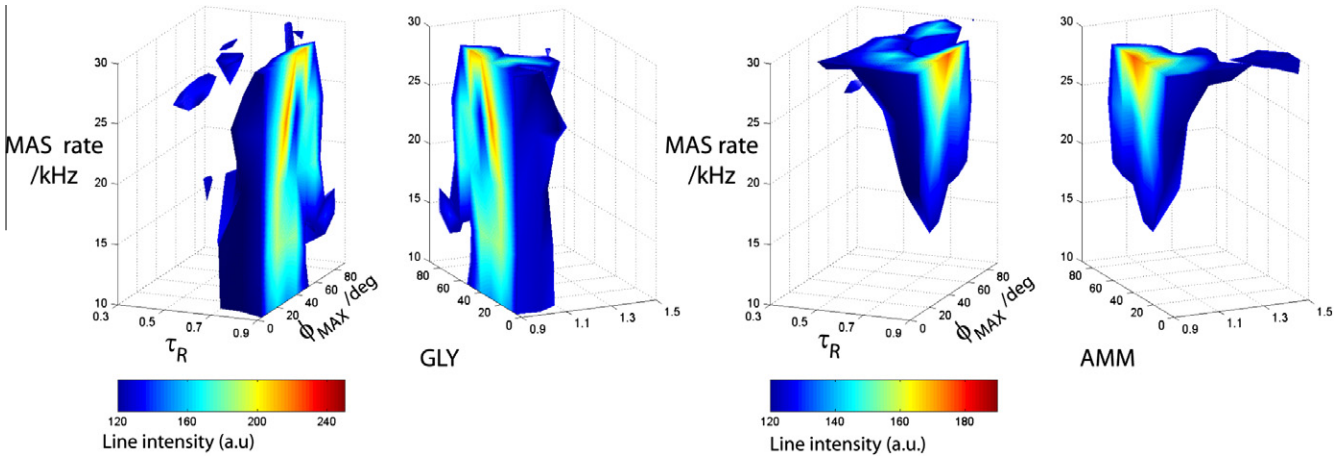

Fig. 2. Graphical representation of the gain in decoupling performance of TPPM over CW. On two carbon sites (GLY on the left and AMM on the right-hand side), as a function of ϕ_{MAX}, τ_R and of the MAS rate. The volumes encompass the parameter space in which the TPPM produces line intensities of 20% or more higher than CW. The line intensities are normalized to the corresponding CW experiment, set to 100.

over CW, a large selection of modulation parameters ameliorate the outcome of CW at high spinning speeds, up to a factor of almost two in amelioration of TPPM vs. CW decoupling.

Table 3 translates and generalizes the previous comparison, by reporting the fraction of the overall parametric volume for which a given method produces at least 20% more intensities than CW, for all molecules. Since the CW response of our samples degrades differently with MAS (Table 2), we reported separately the specific behavior at the spinning frequency of 10 kHz (Table 3A), as well as the global performance over the ensemble of five spinning rates (Table 3B). The variations of the performance of the phase-modulated methods as a function of the molecular system are rather dramatic. Best results are obtained for the case of tyrosine, where up to 58% of the parametric volume explored was effective (for the GT2 method) in improving considerably over CW. Incidentally tyrosine is one of the most common test samples for proton decoupling. This system is also the one for which CW lineshapes degrade the fastest with increasing MAS rates (Table 2). On the other end of the scale we may place AMM, for which CW at high MAS frequencies is still providing good performances, and for which concurrently phase-modulated methods do not improve much on it. For GLY and PSA, although both being a CH_2 unit, the CW behavior seems different, PSA degrading faster. However, the response to phase-modulated pulses (relative to CW) is very similar. The outstanding exception to the general trend is AMM at 10 kHz MAS, where little improvement in the decoupling outcome is achieved through phase-modulated pulses. This is probably due to the facile first-stage (i.e. for the narrow component) decoupling obtained for this molecule, as Table 1 shows that AMM indeed possesses the longest observed T_2' (twice as long as the other ones) even in not optimized conditions. Finally, it can be observed GTn methods produce a great improvement in terms of a broader range of stability with respect to TPPM.

Table 3
Decoupling efficiency of phase-modulated pulses vs. CW irradiation. Fraction of the explored parameter space (see Fig. 2) for which a given phase-modulated method outperforms CW irradiation of at least 20%. A. MAS rate of 10 kHz B. Sum over MAS rates from 10 to 30 kHz.

System	Pulse			
	TPPM (%)	GT2 (%)	GT4 (%)	GT8 (%)
Panel A				
TYRb	18	54	50	30
TYRa	11	32	34	20
GLY	10	41	38	23
PSA	5	38	33	20
AMM	0	0	0	0
Panel B				
TYRb	34	58	53	41
TYRa	28	50	47	37
GLY	16	34	28	20
PSA	9	25	25	16
AMM	8	9	12	7

3.5. Best decoupling parametrization

The final aspect to explore is the variation of the optimal phase modulation parametrization over the studied systems and decoupling pulses. Fig. 3 summarizes the outcome of the best decoupling coordinates found in our parametric search for the tested molecules and methods. Intensity values were normalized as explained in the methods section. The top panels represents the best decoupling achieved, in terms of normalized intensity of the carbon signal, as a function of the spinning rate. In the bottom panels we show the value of the phase jump for which this maximum value of the intensities were attained, for any given MAS frequency. In almost all cases the best reduced period of modulation was found to be at 0.92. The exception is the GT2 pulse, which shows a few local maxima of similar associated intensity, the best one being at a value of 1.04 for the reduced period. In this case 0.92 is one of the secondary maxima. This is in agreement with previous studies and partial theoretical explanations, which find usually the best

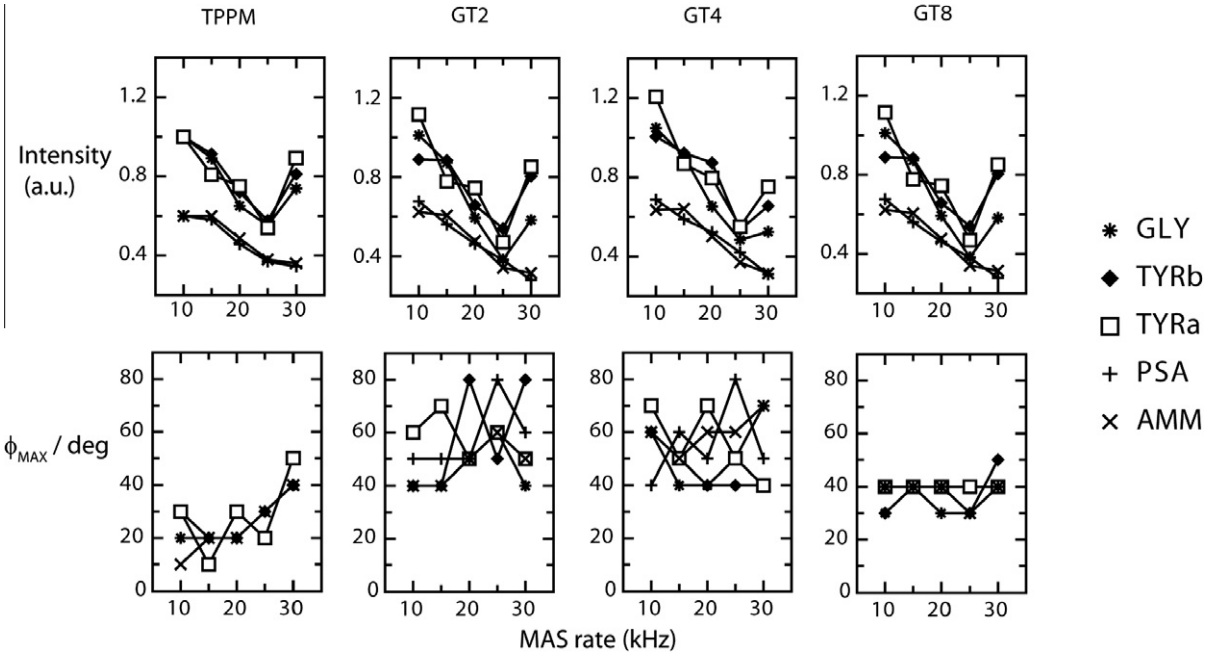

Fig. 3. Evolution of optimal decoupling performance with increasing the MAS rate, for on-resonance decoupling measured on the five systems of Fig. 1. Top panels: line intensity vs. MAS rate. For each system, the intensity values are referenced to the 10 kHz MAS rate experiment. Slightly different normalization values were used for each system for the sake of readability. Bottom panels: optimal phase jump ϕ_{MAX} vs. MAS rate. Results for the four decoupling pulses (TPPM, GT2, GT4, GT8) are from the right to the left. In almost all cases the best reduced period, τ_{TPPM}/τ_{RF}, was found to be 0.92 (see text).

phase-modulation period close to the RF one [3,19,25]. However, our sampling in this dimension is not fine enough to exclude the presence of more localized maxima.

To account for the many sources of refocussable linewidths (see above), we concentrate our analysis on variations in line intensities, rather than on their absolute values. For clarity of reading of the plots, GLY and TYR line intensities were normalized to 1 for MAS of 10 kHz, while those of AMM and PSA were assigned a value of 0.6.

Inspection of Fig. 3 demonstrates a few clear trends. As expected [15], decoupling is well performing at moderate spinning rates, for all molecules. With respect to increasing MAS rate, the samples divide into two families. While the quality of decoupling for PSA and AMM degrades monotonically with increasing spinning rates, GLY and TYR show an intensity drop up to 25 kHz MAS rate, followed by a recover for 30 kHz. In most cases, augmenting the MAS rate required increasingly wider phase jumps to achieve the best performance (Fig. 3). Since the effectiveness of phase-modulated decoupling depends on the interplay of the proton homonuclear dipolar and CSA interactions, a finer theoretical analysis of the MAS rate dependence of the line intensity would be required to accurately describe the different behavior.

For the case of TPPM and GLY, the best phase jump at 10 kHz is 10–15°, while larger angles of up to 40° are most effective at 30 kHz MAS rate. Similar trends are observed for all the samples of this study. GTn decoupling achieves comparable or better intensities with respect to TPPM, while the associated best phase jump is usually slightly larger. The GT8 pulse presents the most stable behavior with respect to the phase jump, since it remains in the 30–40° range for all MAS frequencies. The other methods (GT2 and GT4) have an intermediate behavior.

The effect of changing the proton irradiation frequency of plus or minus 2 kHz results in a small variation of the line intensities, but the general trend of Fig. 3 is conserved (not shown).

4. Conclusions

We tested a few phase-modulated proton heteronuclear decoupling methods on five carbon sites (three CH_2 and two CH) on four different molecular systems. These latter were classified with respect to their intrinsic proton decoupling attitude by testing the degradation of the CW irradiation efficiency upon increasing the MAS rate.

Phase-modulated methods are most effective for decoupling-resistant molecular systems, according to this scale. Interestingly, this is the case even for moderate spinning rates for which CW decoupling provides exploitable linewidths and intensities. No single set of parameters was found to be optimum for all tested molecules, so that care should be applied in transposing the proton heteronuclear decoupling parametrization optimized on one molecule to an unknown one. It is the amplitude of the phase modulation, rather than its reduced period, that has been found to be most sensitive to the molecular system and to the spinning rate. Among the tested decoupling methods, GT8 provides the most stable conditions in terms of phase-modulation parameterization, and GT4 was found the overall most tolerant to misset. The compounds studied divided in two families, one of which with weak response to phase-modulated methods, with respect to plain continuous-wave irradiation. More complicated molecular systems could carry portions belonging to both families. The differences among the systems studied here are likely to be linked to the evolution of the proton bath structure with the spinning rate, and to its non-ergodic partitioning. This study has no ambition of completeness, but it provides evidence that a proper model for spin dynamics in organic solids resist oversimplification. Particularly, it appears not prudent to generically predict the decoupling behavior on the basis of a given carbon proton multiplicity.

Acknowledgment

We are grateful to the Spectropôle, Fédération de Sciences Chimiques (CNRS FR 1739) de Marseille, for privileged spectrometer time access.

Appendix A

A.1. Synthesis of the phenyl-succinic acid

A new synthetic route was designed to obtain selectively labeled phenyl-succinic acid, according to the following scheme:

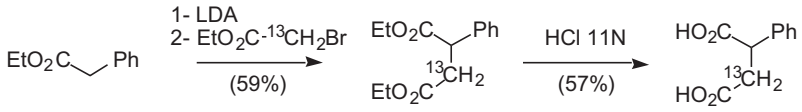

A.2. Diethyl 2-phenylsuccinate-3^{13}C

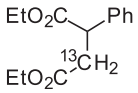

A solution of ethyl phenylacetate (100 mg, 0.61 mmol) in 2 ml of dry THF was cooled at −78 °C. A 2 M LDA solution (350 µl, 0.7 mmol) was slowly added and stirred 1 h at the same temperature. Ethyl 2-bromoacetate-2^{13}C (102 mg, 0.61 mmol) was then added dropwise. The reaction mixture was allowed to warm to room temperature overnight. After dilution with water, the reaction was extracted three times with Et_2O and dried. The solvent was removed in vacuum and the crude material was subjected to column chromatography on silica gel (EtOAc/pentane 0:100 to 5/95) to afford the product (90 mg, 0.36 mmol, 59%). ^1H NMR (300 MHz, $CDCl_3$): 7.30 (m, 5H); 4.25-4.04 (m, 5H); 3.18 (ddd, J^1_{C-H} = 131.5, J^2_{H-H} = 16.8, J^3_{H-H} = 10.0, 1H); 2.66 (ddd, J^1_{C-H} = 130.5, J^2_{H-H} = 16.8, J^3_{H-H} = 5.3, 1H); 1.21 (q, J = 7.4, 6H.%). ^{13}C NMR (75 MHz, $CDCl_3$): 38.3 ($^{13}CH_2$).

A.3. 2-phenyl-succinic acid-3^{13}C

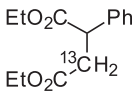

A solution of diethyl 2-phenylsuccinate-3^{13}C (90 mg, 0.36 mmol) in 3 ml of 11 N HCl was refluxed overnight. The solution was then slowly cooled to 0 °C allowing the crystallization of the product. The filtration and drying by vacuo afforded the pure product (40 mg, 0.21 mmol, 57%). ^{1}H NMR (300 MHz, CD_3OD): 7.29 (m, 5H); 4.04 (dt, J = 10.2 and 5.1, 1H); 3.21 (ddd, J^1_{C-H} = 130.7, J^2_{H-H} = 17.0, J^3_{H-H} = 10.2, 1H); 2.64 (ddd, J^1_{C-H} = 129.6, J^2_{H-H} = 17.0, J^3_{H-H} = 5.1, 1H.%). ^{13}C NMR (75 MHz, CD_3OD): 37.7 ($^{13}CH_2$).

References

[1] W.R. Zhang, D.G. Cory, First direct measurement of the spin diffusion rate in a homogenous solid, Phys. Rev. Lett. 80 (1998) 1324–1327.
[2] M. Mehring, Principles of High Resolution NMR in Solids, Springer, Berlin, 1983.
[3] M. Ernst, S. Bush, A.C. Kolbert, A. Pines, Second-order recoupling of chemical-shielding and dipolar-coupling tensors under spin decoupling in solid-state NMR, J. Chem. Phys. 105 (1996) 3387–3397.
[4] A.K. Khitrin, G. McGeorge, B.M. Fung, Heteronuclear Decoupling in Solids, Encyclopedia of Nuclear Magnetic Resonance, John Wiley and Sons, Chichester, 2002.
[5] P. Tekely, P. Palmas, D. Canet, Effect of proton spin-exchange on the residual C-13 Mas Nmr Linewidths – phase-modulated irradiation for efficient heteronuclear decoupling in rapidly rotating solids, J. Magn. Reson., Ser. A 107 (1994) 129–133.
[6] A.E. Bennett, C.M. Rienstra, M. Auger, K.V. Lakshmi, R.G. Griffin, Heteronuclear decoupling in rotating solids, J. Chem. Phys. 103 (1995) 6951–6958.
[7] Z. Gan, R.R. Ernst, Frequency- and phase-modulated heteronuclear decoupling in rotating solids, Solid State NMR 8 (1997) 153–159.
[8] H. Geen, A.S.D. Heindrichs, J.J. Titman, M. Ernst, B.H. Meier, Investigation of the feasibility of amplitude-modulated dipolar decoupling in magic-angle spinning solid-state nuclear magnetic resonance, J. Phys. Chem. B – Atom. Mol. Opt. Phys. (2000) 3377–3391.
[9] K. Takegoshi, J. Mizokami, T. Terao, H-1 decoupling with third averaging in solid NMR, Chem. Phys. Lett. 341 (2001) 540–544.
[10] B.M. Fung, A.K. Khitrin, K. Ermolaev, An improved broadband decoupling sequence for liquid crystals and solids, J. Magn. Reson. 142 (2000) 97–101.
[11] A. Khitrin, B.M. Fung, Design of heteronuclear decoupling sequences for solids, J. Chem. Phys. 112 (2000) 2392–2398.
[12] A.K. Khitrin, T. Fujiwara, H. Akutsu, Phase-modulated heteronuclear decoupling in NMR of solids, J. Magn. Reson. 162 (2003) 46–53.
[13] A. Detken, E.H. Hardy, M. Ernst, B.H. Meier, Simple and efficient decoupling in magic-angle spinning solid-state NMR: the XiX scheme, Chem. Phys. Lett. 356 (2002) 298–304.
[14] G. De Paepe, D. Sakellariou, P. Hodgkinson, S. Hediger, L. Emsley, Heteronuclear decoupling in NMR of liquid crystals using continuous phase modulation, Chem. Phys. Lett. 368 (2003) 511–522.
[15] G. Gerbaud, F. Ziarelli, S. Caldarelli, Increasing the robustness of heteronuclear decoupling in magic-angle sample spinning solid-state NMR, Chem. Phys. Lett. 377 (2003) 1–5.
[16] K. Riedel, J. Leppert, O. Ohlenschlager, M. Gorlach, R. Ramachandran, Heteronuclear decoupling in rotating solids via symmetry-based adiabatic RF pulse schemes, Chem. Phys. Lett. 395 (2004) 356–361.
[17] R.S. Thakur, N.D. Kurur, P.K. Madhu, Swept-frequency two-pulse phase modulation for heteronuclear dipolar decoupling in solid-state NMR, Chem. Phys. Lett. 426 (2006) 459–463.
[18] M. Weingarth, G. Bodenhausen, P. Tekely, Low-power decoupling at high spinning frequencies in high static fields (low-power PISSARRO), J. Magn. Reson. 199 (2009) 238–241.
[19] M. Edén, M.H. Levitt, Pulse sequence symmetries in the nuclear magnetic resonance of spinning solids: application to heteronuclear decoupling, J. Chem. Phys. 111 (1999) 1511–1519.
[20] G. De Paepe, N. Giraud, A. Lesage, P. Hodgkinson, A. Bockmann, L. Emsley, Transverse dephasing optimized solid-state NMR spectroscopy, J. Am. Chem. Soc. 125 (2003) 13938–13939.
[21] G. De Paepe, P. Hodgkinson, L. Emsley, Improved heteronuclear decoupling schemes for solid-state magic angle spinning NMR by direct spectral optimization, Chem. Phys. Lett. 376 (2003) 259–267.
[22] R.S. Thakur, N.D. Kurur, P.K. Madhu, An analysis of phase-modulated heteronuclear dipolar decoupling sequences in solid-state nuclear magnetic resonance, J. Magn. Reson. 193 (2008) 77–88.
[23] I. Scholz, P. Hodgkinson, B.H. Meier, M. Ernst, Understanding two-pulse phase-modulated decoupling in solid-state NMR, J. Chem. Phys. 130 (2009) 114510–114517.
[24] M. Ernst, Heteronuclear spin decoupling in solid-state NMR under magic-angle sample spinning, J. Magn. Reson. 162 (2003) 1–34.
[25] G. De Paepe, B. Elena, L. Emsley, Characterization of heteronuclear decoupling through proton spin dynamics in solid-state nuclear magnetic resonance spectroscopy, J. Chem. Phys. 121 (2004) 3165–3180.
[26] M. Leskes, R.S. Thakur, P.K. Madhu, N.D. Kurur, S. Vega, Bimodal Floquet description of heteronuclear dipolar decoupling in solid-state nuclear magnetic resonance, J. Chem. Phys. 127 (2007).
[27] R. Ramachandran, V.S. Bajaj, R.G. Griffina, Theory of heteronuclear decoupling in solid-state nuclear magnetic resonance using multi pole-multimode Floquet theory, J. Chem. Phys. 122 (2005).
[28] G. Metz, X.L. Wu, S.O. Smith, Ramped-amplitude cross polarization in magic-angle-spinning NMR, J. Magn. Reson. A 110 (1994) 219–227.
[29] C. Di Pietro, S. Campagna, V. Ricevuto, M. Giannetto, A. Manfredi, G. Pozzi, S. Quici, Synthesis, photophysical properties, and complexation behavior of three new luminescent tetraaza-tetraoxamacrobicyclic receptors, J. Org. Chem. (2001) 587–594.
[30] D.L. VanderHart, G.C. Campbell, A close look at13C CPMAS linewidths in solids for rigid, strongly coupled carbons under CW proton decoupling, J. Magn. Reson. 134 (1998) 88–112.
[31] M.J. Potrzebowski, P. Tekely, Y. Dusausoy, Comment to C-13-NMR studies of alpha and gamma polymorphs of glycine, Solid State Nucl. Magn. Reson. 11 (1998) 253–257.
[32] Z.T. Gu, K. Ebisawa, A. McDermott, Hydrogen bonding effects on amine rotation rates in crystalline amino acids, Solid State Nucl. Magn. Reson. 7 (1996) 161–172.
[33] J.R. Sachleben, S. Caldarelli, L. Emsley, The effect of spin decoupling on line shapes in solid-state nuclear magnetic resonance, J. Chem. Phys. 104 (1996) 2518–2528.